blood®
Regular Article

Check for updates

MYELOID NEOPLASIA

Disrupting tRNA modifications to target mitochondrial vulnerabilities in drug-resistant leukemia cells

Cornelius Pauli,[1-3,*] Michael Kienhöfer,[1,2,*] Maximilian Felix Blank,[2-4] Oguzhan Begik,[5] Christian Rohde,[2,3] Sarah Miriam Naomi Zimmermann,[3,4] Laura Werner,[2] Daniel Heid,[2,3] Fu Xu,[1] Katharina Weidenauer,[2] Sylvain Delaunay,[1] Nadja Krall,[1,2] Katrin Trunk,[1] Duoduo Zhao,[2,3] Fengbiao Zhou,[2,3] Laia Llovera,[5] Alexane Ollivier,[5] Anke Heit-Mondrzyk,[1] Uwe Platzbecker,[6] Claudia Baldus,[7] Hubert Serve,[8] Martin Bornhäuser,[9] Cathrine Broberg Vågbø,[10] Salvador Aznar Benitah,[11,12] Jeroen Krijgsveld,[4,13] Eva Maria Novoa,[5,12,14] Carsten Müller-Tidow,[2,3] and Michaela Frye[1]

[1]Division of Mechanisms Regulating Gene Expression, German Cancer Research Center, Heidelberg, Germany; [2]Medical Faculty Heidelberg and Department of Internal Medicine V, Heidelberg University Hospital, Heidelberg, Germany; [3]Molecular Medicine Partnership Unit European Molecular Biology Laboratory–University Hospital Heidelberg, European Molecular Biology Laboratory, Heidelberg, Germany; [4]Division of Proteomics of Stem Cells and Cancer, German Cancer Research Center, Heidelberg, Germany; [5]Epitranscriptomics and RNA Dynamics, Centre for Genomic Regulation, The Barcelona Institute of Science and Technology, Barcelona, Spain; [6]Department of Hematology, Leipzig University Hospital, Leipzig, Germany; [7]Department of Hematology, Kiel University Hospital, Kiel, Germany; [8]Department of Hematology, Frankfurt University Hospital, Frankfurt, Germany; [9]Department of Hematology, Dresden University Hospital, Dresden, Germany; [10]Proteomics and Modomics Experimental Core Facility, Norwegian University of Science and Technology and St. Olavs Hospital, Trondheim, Norway; [11]Aging and Metabolism, Institute for Research in Biomedicine, The Barcelona Institute of Science and Technology, Barcelona, Spain; [12]Catalan Institution for Research and Advanced Studies, Barcelona, Spain; [13]Medical Faculty, Heidelberg University, Heidelberg, Germany; and [14]Universitat Pompeu Fabra, Barcelona, Spain

KEY POINTS

- **TRMT5-mediated N1-methylguanosine tRNA modifications drive mitochondrial function and drug tolerance in AML via oxidative phosphorylation.**
- **TRMT5 inhibition prevents oxidative phosphorylation upregulation and synergizes with cytarabine and Ven to overcome resistance.**

Dysregulated RNA modifications contribute to cancer progression and therapy resistance, yet the underlying mechanism often remains unknown. Here, we perform CRISPR-based synthetic lethality screens to systematically explore the role of RNA modifications in mediating resistance to antileukemic drugs. We identify the tRNA methyltransferase 5 (TRMT5)–mediated formation of N1-methylguanosine (m^1G) in the transfer RNA (tRNA) anticodon loop as essential for mediating drug tolerance to cytarabine and venetoclax (Ven) in acute myeloid leukemia (AML). TRMT5 methylates nearly all mitochondrial and nuclear tRNAs with a guanosine at position 37, but its role in promoting drug tolerance specifically depends on its mitochondrial function. TRMT5 is essential for the dynamic upregulation of mitochondrial messenger RNA translation and oxidative phosphorylation, which are critical for sustaining drug tolerance in leukemia cells. This mitochondrial dependency correlates with therapy outcomes in patients with leukemia: lower expression of electron transport chain genes is linked to poorer outcomes in a cohort of nearly 100 patients with AML undergoing first induction therapy. Finally, we demonstrate that targeted depletion of the TRMT5 protein using a conditional degron, in conjunction with cytarabine and Ven treatment, synergistically induces cell death in drug-tolerant AML cells. Thus, our study reveals TRMT5 as a promising drug target for therapy-resistant leukemia.

Introduction

RNA biochemical modifications regulate gene expression by affecting RNA stability, nuclear export, localization, and translation.[1] Their cellular function is best studied during acute stress responses,[2-4] where RNA-modifying proteins (RMPs) either degrade or stabilize their target RNAs to rewire cellular proteomes, often even before transcriptional changes occur.[5-7] Thus, RNA modifications sense alterations in the environment and initiate cellular stress responses accordingly.

The ability to adapt to a changing microenvironment is crucial for cell fate decisions during development. Aberrant deposition of RNA modifications is frequently linked to human diseases such as neurological deficits and metabolic disorders.[1,4] Similarly, cancer cells continually and dynamically adapt to often deleterious microenvironments, induced by factors such as hypoxia or drug treatments.[8] Accordingly, RNA modifications have been found to play biological roles in most cancers by regulating fundamental cellular processes such as growth, survival, differentiation, and migration.[3,9] Consequently, most

Downloaded from http://ashpublications.org/blood/article-pdf/146/20/2443/2420053/blood_bld-2024-027822-main.pdf by guest on 20 March 2026

aspects of tumorigenesis, including initiation, growth, metastasis and therapy resistance, can require distinct RNA-modifying events to ensure cell survival and growth.[1,3]

Here, we performed CRISPR-based synthetic lethality screens targeting all currently known 150 RMPs.[10] We demonstrate that drug-tolerant leukemia cells require tRNA methyltransferase 5 (TRMT5)–mediated formation of N1-methylguanosine (m^1G) in mitochondrial transfer RNA (mt-tRNAs) to survive exposure to cytarabine or venetoclax (Ven); both drugs are frequently used in the treatment of patients with acute myeloid leukemia (AML). The loss of m^1G impaired mitochondrial messenger RNA (mt-mRNA) translation and reduced respiration, and thereby resensitized drug-tolerant cells to cytarabine. Although TRMT5 methylates both mt-tRNAs and nuclear-encoded tRNAs, selectively inhibiting its function in mitochondria alone was sufficient to enhance the cancer drug's toxicity. Finally, we demonstrate that mitochondrial activity not only predicted therapy outcome in patients with leukemia but also represented a targetable vulnerability. TRMT5 inhibition significantly amplified the efficacy of Ven and cytarabine treatment in resistant cells. In summary, disrupting TRMT5-mediated tRNA methylation is a promising strategy to enhance leukemia treatment or minimize side effects of cancer drug treatments.

Materials and methods

CRISPR-based dropout screens

A CRISPR-Cas9 library consisting of single-guide RNAs (sgRNA) targeting 150 RMPs and 8 control genes (8 sgRNAs per protein), 250 small nucleolar RNAs (~2 sgRNAs per small nucleolar RNA), and 50 nontargeting sgRNAs was designed. The 1708 sgRNAs were cloned into the lentiCRISPRv2–green fluorescent protein (GFP) vector (82461, Addgene). The sgRNA-bearing plasmids were transduced together with the lentiviral envelope plasmid pDM2g (12259, Addgene) and the packaging plasmid psPAX2 (12260, Addgene) into lenti-X 293T cells using TurboFect transfection reagent (R0531, Thermo Fisher Scientific). Lentiviruses were harvested after 72 hours and concentrated via ultracentrifugation. Before infection, virus concentration was titrated to a multiplicity of infection of 0.3.

The cell lines were infected and samples were taken after 48 hours (input; day 1), 8 days, and 22 days. For the synthetic lethal screen, Ontario Cancer Institute–Acute Myeloid Leukemia Line 2 (OCI-AML2) cells were GFP sorted 96 hours after infection and then divided into treatment and control groups. The treatment group was stimulated for 3 days with cytarabine (STADA) followed by 4 days for recovery. Furthermore, 3 treatment-recovery cycles were performed with increasing doses of cytarabine (1 μM, 2 μM, 3 μM). Samples were taken on days 8, 15, and 22.

sgRNA sequencing and quantification

The whole genomic DNA was isolated using the Quick-DNA Midiprep Plus Kit (Zymo Research). Polymerase chain reaction (PCR) input amount was concentrated to achieve a 500× coverage. Library preparation and sequencing was performed as described previously.[11,12] After sequencing on an Illumina NextSeq500, the reads were demultiplexed using the P7 barcode in addition to the in-line barcode information. Each read was scanned for the vector motif, and the subsequent 20 nucleotides were used to assign 1 of the 1708 unique sgRNAs from the screen. The robust ranking aggregation algorithm in model-based analysis of genome-wide CRISPR/Cas9 knockout (MAGeCK) software version 0.5.9.4 was used to identify positively or negatively enriched guide RNAs (gRNAs).

TRMT5 knockout and rescue constructs

The coding sequence of TRMT5 isoform 3 was cloned into an pCDH-EF1α-MCS-(PGK-GFP) plasmid (CD811A-1, System Biosciences). The target sequence for sgRNA2, along with the corresponding protospacer adjacent motif (PAM), was silently mutated via PCR-based mutagenesis. To generate a catalytically inactive version of TRMT5, point mutations were introduced at 3 catalytically critical amino acids (E288A, R291H, M386V).[13] The mitochondrial targeting sequence (MTS) was identified using the internal MTS-like sequences (iMTS) score (https://mtsviewer.neurohub.ca/)[14] and removed from the coding sequence using mutagenesis PCR.

Nanopore sequencing

Native tRNAs were sequenced using nanopore tRNA sequencing.[15] The library was loaded onto MinION R9.4 flow cells (FLO-MIN-106). Reads were base called using Guppy version 3.6.1 in high-accuracy mode. Reads were mapped using Burrows-Wheeler Aligner (arXiv:1303.3997v2) with parameters *bwa mem -W13 -k6 -xont2d -T20* to the mature human tRNA reference set, obtained from gtRNAdb 2.0,[16] to which we added the ligated adapter sequences. Differential tRNA modifications were analyzed by extracting basecalling "errors" (mismatch, insertion, and deletion) for each position, using the *get_sum_err.py* script. The output of this script was then used to calculate differential summed "errors" between wild-type (WT) and TRMT5 knockout (KO) samples, which were visualized using the *plot_heatmap.py* script. Both scripts are publicly available in GitHub (https://github.com/novoalab/Nano-tRNAseq).

Total and nascent proteomics

Cells were grown at equal density overnight. GFP-sorted TRMT5 KO and control (scramble) cells were harvested on days 12 and 13 after infection. Furthermore, 4×10^6 cells per condition and replicates were washed thrice with ice-cold 1× phosphate-buffered saline. Experiments were conducted at least in triplicates. Raw data were processed with MaxQuant (1.6.2.6)[17] using default settings. Only proteins with at least 1 unique peptide were considered as identified, and normalized label-free quantification values were used for quantitative comparative analyses. Nascent proteomics studies were performed as described previously.[18]

TRMT5-inducible degron system

For TRMT5-specific protein degradation, we used the degradation TAG (dTAG) system.[19] For the in-frame knockin of $FKBP12^{F36V}$, an electroporation-based approach was used using the Neon Transfection System. A total of 1250 ng of recombinant Cas9 (A36498, Thermo Fisher Scientific) was incubated with 7.5 pmol of CRISPR RNA for 10 minutes and subsequently mixed with 200 ng of donor DNA containing $FKBP12^{F36V}$-2xHA-T2A-mCherry (eu.idtdna.com). The reaction mixture was added to 2.5×10^5 cells resuspended in buffer R, corresponding to a concentration of $20 \times 10^3/\mu L$. Electroporation was carried out under 3 different conditions (1600 V/10 ms/3 pulses, 1700 V/20 ms/1 pulse, 1150 V/30 ms/2 pulses), and cells were pooled in prewarmed medium supplemented with 2 μM

Downloaded from http://ashpublications.org/blood/article-pdf/146/20/2443/2420053/blood_bld-2024-027822-main.pdf by guest on 20 March 2026

ROCK inhibitor (SCM075, Sigma-Aldrich). After 72 hours, mCherry-positive cells were single-cell sorted into 96-well plates. After 16 days, successfully outgrown single clones were screened for homologous knockins via gel electrophoresis of amplified TRMT5 DNA. For functional assays, TRMT5 degradation was induced using varying concentrations of dTAG-V1 (7374, Tocris Bioscience).

Data availability

Data in supplemental Table 13 (available on the *Blood* website) were obtained from Stratman et al.[20] Results are in part based on DepMap[21] and the Cancer Cell Line Encyclopedia.[22]

A detailed "Materials and methods" description is provided as a supplemental File.

Results

Target discovery screen identifies essential RNA modifications in cancer cells

To identify cancer-relevant RNA modifications, we generated pooled gRNA libraries targeting all currently known human RMPs (n = 150) (supplemental Figure 1A; supplemental Table 1).[10] After extensive quality checks (supplemental Figure 1B-I), we performed dropout viability screens in 16 different cancer cell lines and 2 primary healthy lines (supplemental Table 2).

Approximately one-third of RMP-targeting gRNAs were significantly depleted after 22 days of culture (Figure 1A; supplemental Table 3A-B). Similar to the MYC proto-oncogene, bHLH transcription factor (MYC), TRMT112 was essential for survival of all cell lines (Figure 1A). TRMT112 forms heterodimer with methyltransferase 5 (METTL5) or THUMP domain 3 tRNA guanosine methyltransferase (THUMPD3) to form N6-methyladenosine (m^6A) in 18S ribosomal RNA and m^2G in cytoplasmic tRNAs, respectively.[23,24] Only a small number of gRNAs, such as the control gRNAs targeting the tumor suppressor TP53, were enriched, indicating a growth advantage when the targeted RMP was depleted (Figure 1A). We obtained a similar dependency on RMPs after 8 days of culture (supplemental Figure 1J-K). The gene effects observed in our CRISPR screen closely correlated with genome-scale CRISPR dropout screens performed in >1000 cancer lines (Figure 1B; depmap.org).[25] In total, we identified 50 essential RMPs required for cellular survival in at least 1 of the 18 tested cell lines (https://shiny-portal.embl.de/shinyapps/app/15_rnamod_trmt5).

Synthetic lethality screen identifies essential roles of TRMT5 in cancer drug tolerance

RNA modifications are often linked to cellular stresses such as oxidative stress, DNA damage, or drug treatment. To identify cancer stress-specific modifications, we conducted synthetic lethality screens between RNA modifications and anticancer drugs. After treating 5 different AML cell lines with cytarabine (AraC), we found that OCI-AML2 and OCI-AML3 cells exhibited a >100-fold greater tolerance to AraC compared with other tested lines (Figure 1C). The OCI-AML2 line was then used for the synthetic lethality screen. After infection of the CRISPR library, the cells were repeatedly exposed to AraC in an increasing concentration (Figure 1D-E). To exclude RMPs frequently required for cell survival and proliferation, we compared treated with untreated cells both cultured for 22 days (Figure 1F; supplemental Figure 1L).

The sgRNAs targeting TRMT5 and CTU2 were the most significantly depleted (Figure 1F; supplemental Figure 1L-M). The averaged MAGeCK-negative enrichment score revealed a similarly significant reduction of gRNAs targeting TRMT5 and CTU2 (Figure 1G). Both enzymes modify the tRNA anticodon loop. Although CTU2 is responsible for 2-thiolation of cytosolic tRNAs, TRMT5 methylates the N1 position of guanosine 37 (G37) in mt-tRNAs.[13,26,27] We chose TRMT5 for further analyses because its protein expression significantly correlated with half maximal 50% inhibitory concentrations of AraC in blood cancer cells, which was not the case for CTU2 (Figure 1H; supplemental Figure 1N).[28] Although KO of TRMT5 caused a negative gene effect across 1178 cancer lines (Figure 1B,I), its correlation with AraC sensitivity was lineage specific and included lymphoid and myeloid blood cancer cells (Figure 1J).

TRMT5 forms m^1G at position 37 in mitochondrial and cytosolic tRNAs

To identify TRMT5-specific methylation targets, we selected 2 sgRNAs (sg2 and sg4) and generated 2 drug-tolerant (OCI-AML2, OCI-AML3) and 2 drug-sensitive (MOLM13, Kasumi) KO lines (supplemental Figure 2A). We isolated mt-tRNAs and measured a twofold reduction of m^1G levels in TRMT5-KO cells by mass spectrometry (Figure 2A-B). The residual levels of m^1G in KO cells were likely due to tRNA modifications at position 9, mediated by TRMT10A.[29] Therefore, we next quantified m^1G37 levels in their sequence-specific context using nanopore direct RNA sequencing.[15] This method efficiently detected m^1G in synthetic modified mt-$tRNA^{Leu}$, a known target of TRMT5 (supplemental Figure 2B-D; supplemental Table 4).[13] Then, we compared the modification profiles of mitochondrial and cytosolic tRNAs. Most G37-containing tRNAs demonstrated highly reproducible reductions in m^1G levels when TRMT5 was depleted, whereas all other tRNAs were unaffected (Figure 2C-G; supplemental Figure 2E; supplemental Table 5).

Next, we rescued TRMT5-KO cells with constructs expressing either the WT or a catalytic dead (mutant) versions of the protein.[13] In addition, we generated a TRMT5 construct lacking the predicted mitochondrial transfer peptide (ΔMTS), making it unable to shuttle into the mitochondria (Figure 2H-I). Most G37 methylation sites were rescued by reexpressing the WT but not the nonfunctioning proteins, confirming that the reduction of m^1G37 levels was directly caused by loss of TRMT5 (Figure 2J; supplemental Figure 2F-H; supplemental Table 6). Although reexpression of the ΔMTS-TRMT5 protein failed to rescue mt-tRNA methylation, it increased methylation of cytosolic tRNAs when compared with the catalytic-dead protein (Figure 2J). We concluded that human TRMT5 methylates both mitochondrial- and nuclear-encoded tRNAs at position G37.

TRMT5 is required for efficient mRNA translation of OXPHOS components

Mitochondrial activity and high oxidative phosphorylation (OXPHOS) status are hallmarks of AraC-resistant persisting leukemia cells.[30] Upregulation of OXPHOS requires increased translation of mitochondrial-encoded genes, and modifications in the mt-tRNA anticodon loop ensure efficient codon-specific translation.[31] The m^1G modification next to the

Downloaded from http://ashpublications.org/blood/article-pdf/146/20/2443/2420053/blood_bld-2024-027822-main.pdf by guest on 20 March 2026

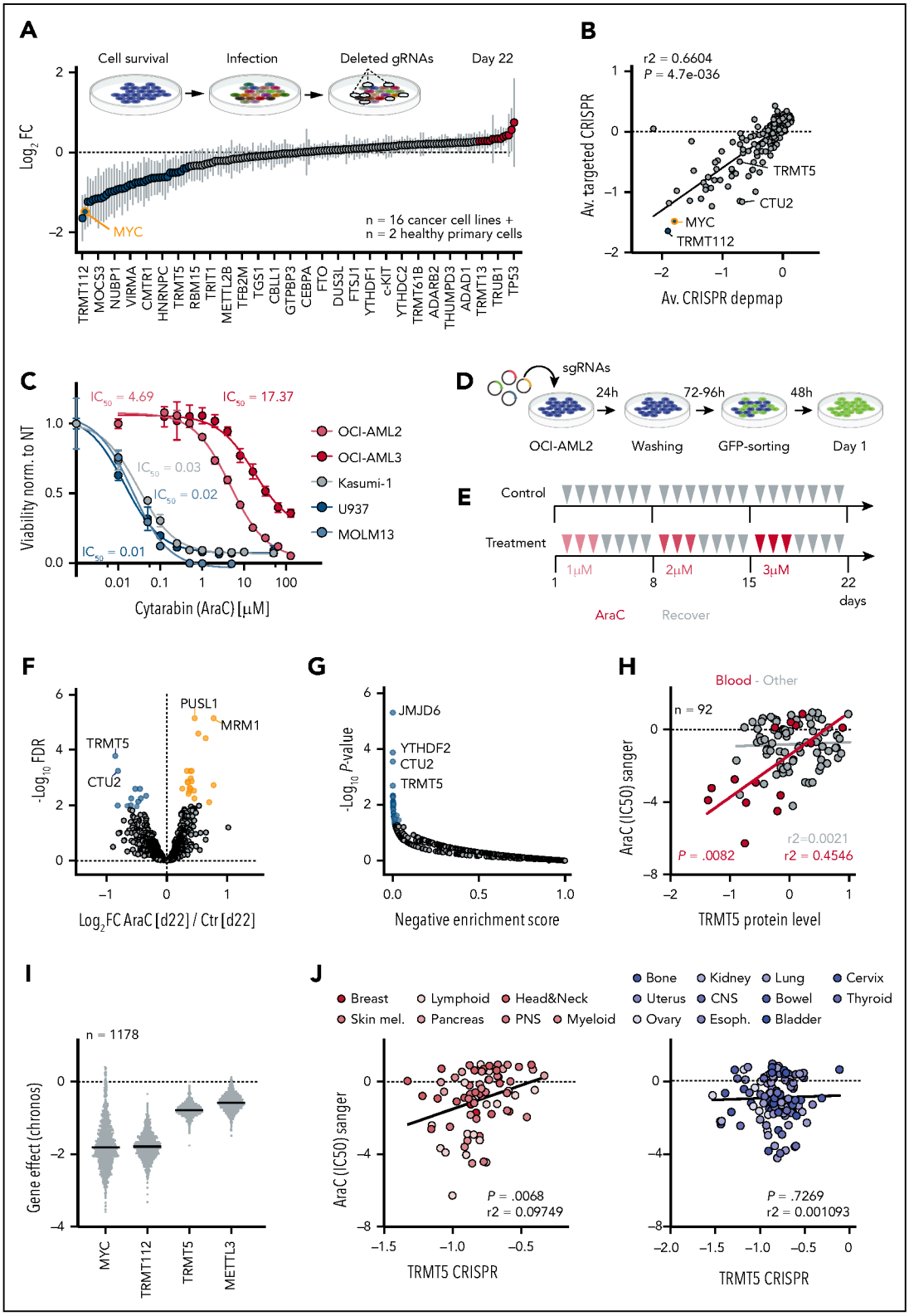

Figure 1. CRISPR/Cas9 genetic screen identifies cancer-relevant RNA modification. (A) Scheme of dropout screen (top) and average log_2 FC (bottom) of 150 human RMPs, including positive controls (Ctrs) in 18 cell lines at day 22 of the experiment. Illustrated is every sixth RMP. (B) Correlation of RMP gene effect in targeted CRISPR experiments and genome-scale CRISPR (Chronos) (depmap.org). Each dot represents the average effect across all tested cell lines. (C) Dose-response curve evaluating the effect of different concentrations of cytarabine (AraC) in blood cancer lines with corresponding IC_{50} values. (D-E) Illustration of synthetic lethality screen (D) and treatment regimen with AraC (E) in OCI-AML2 cells. (F-G) Volcano plot illustrating log_{10} statistical significance (FDR) vs log_2 FC of sgRNA abundance (F) and MAGeCK-negative enrichment score of averaged gRNAs per gene (G) identifying essential RMPs in AraC-treated cells after 22 days in culture. (H) Correlation between TRMT5 protein expression and IC_{50} values in response to AraC treatment (Sanger, GDSC1) in lymphoid and myeloid cancer lines (blood) and all other cell lines. (I) CRISPR MYC, TRMT112, TRMT5, and METTL3 gene effects (Chronos) (depmap.org) across 1150 cancer cell lines. (J) Cancer lines with significant (left) and nonsignificant (right) correlation of CRISPR TRMT5 gene effect and IC_{50} values of AraC treatment. FC, fold-change; FDR, false discovery rate; IC_{50}, 50% inhibitory concentration.

Downloaded from http://ashpublications.org/blood/article-pdf/146/20/2443/2420053/blood_bld-2024-027822-main.pdf by guest on 20 March 2026

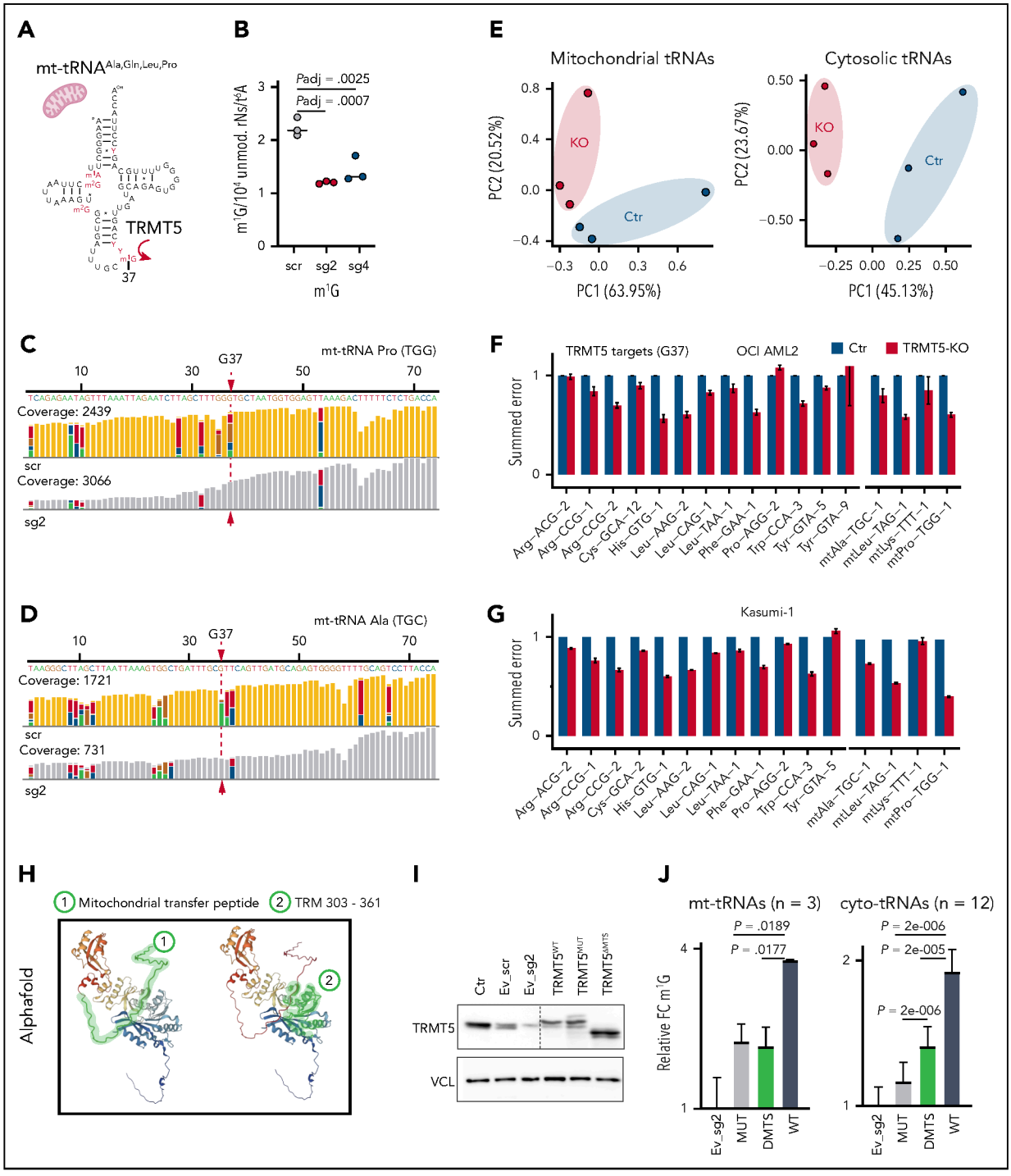

Figure 2. TRMT5 methylates mitochondrial (mt) and cytosolic (cyto) tRNAs at position 37. (A-B) Illustration of mt-tRNAs methylated by TRMT5 at position G37 (A) and quantification of m^1G levels in mt-tRNAs using mass spectrometry (B). Modification levels are normalized to N6-threonyl-carbamoylation, a universal modification of adenosine 37 in tRNAs. (C-D). Integrative genomics viewer snapshot of nanopore sequenced mt-tRNA$^{Pro(TGG)}$ (C) and mt-tRNA$^{Ala(TGC)}$ (D) from OCI-AML2 Ctr (scr; top) and TRMT5- KO (sg2) cells. Nucleotides with mismatch frequencies >0.05 are in color (panels C-D) and in gray otherwise. (E) Principal component analysis of summed error values from mitochondrial (left) and cyto (right) tRNAs in OCI-AML2 Ctr and KO cells. N = 3 infections per conditions. (F-G) Relative summed error of all potential TRMT5 targets (G37) in KO cells compared with Ctr in OCI-AML2 (F) and Kasumi-1 (G) cells. (H) Alpha-fold model predicting TRMT5 protein structure. Green highlights the predicted mitochondrial transfer peptide (left; 1) and the TRM (right; 2). (I) Western blot detecting TRMT5 protein levels in Ctr and rescued TRMT5 KO cells. Cells were infected with scr or sg2. KO cells were rescued by reexpressing TRMT5 WT, catalytic dead (mutant [MUT]) or lacking the MTS constructs. Ctr cells (sg2 and scr) were rescued with an empty vector (EV) Ctr. Vinculin (VCL) serves as a loading Ctr. Dotted line indicates different exposure times of the same blot. (J) FC of relative summed error in TRMT5 mt (n = 3) and (cyto; 12) tRNA targets in the indicated rescued TRMT5 KO lines. Mean ± standard deviation (panels F-G). Mean ± standard error (panel J). Two-tailed paired *t* test (panel J). TRM, tRNA methylation motif.

Downloaded from http://ashpublications.org/blood/article-pdf/146/20/2443/2420053/blood_bld-2024-027822-main.pdf by guest on 20 March 2026

anticodon prevents translational frameshifting (supplemental Figure 3A).[32]

To quantify mt-mRNA translation, we measured OP-puromycin incorporation into elongating polypeptide chains using flow cytometry (Figure 3A). Depletion of TRMT5 reduced mitochondrial protein synthesis in all tested cells (Figure 3B; supplemental Figure 3B). Consequently, basal and maximal oxygen consumption rates (OCRs) decreased in TRMT5-KO cells, but the number of active mitochondria was unaffected (Figure 3C-D; supplemental Figure 3C). Cytoplasmic protein synthesis was also reduced in the absence of TRMT5 (supplemental Figure 3D), and quantitative proteome analyses revealed a significant reduction of electron transport chain (ETC) proteins and an increase in proteins involved in stress responses (supplemental Figure 3E-F; supplemental Table 7). Thus, TRMT5 was required for optimal use of OXPHOS for energy production and protein synthesis.

Drug-tolerant cells switch from low to high OXPHOS in acute stress conditions

Although high OXPHOS levels have been linked to chemotherapy resistance in vivo,[30] we unexpectedly observed that drug-tolerant cancer cells, on average, exhibited the lowest levels of mitochondrial protein expression (MitoCarta3.0; n = 1136) and had comparably low levels of OCRs (supplemental Figure 3G-H; supplemental Table 8). One possible explanation for our observation was that the steady-state growth of drug-tolerant cells might not rely primarily on mitochondria. When we investigated on how acute AraC exposure affected mitochondrial function, we indeed found that only drug-tolerant cells upregulated their OCRs (Figure 3E-F). TRMT5-depleted drug-tolerant cells failed to upregulate OCRs after exposure to AraC, an effect that was rescued by reexpressing the TRMT5 protein (Figure 3G-H), but not the catalytic-dead or mitochondrial-deficient proteins (Figure 3I-J). Nascent proteome analyses revealed that exposure to AraC enhanced expression of virtual all mitochondrial proteins (MitoCarta3.0), yet only in drug-tolerant cells (Figure 3K; supplemental Figure 3I, yellow lines). This activation of mitochondrial protein synthesis depended on the presence of TRMT5 (Figure 3K, blue and red lines; supplemental Table 9A-H). In conclusion, drug-tolerant OCI-AML2 cells required TRMT5-mediated mt-tRNA methylation to activate mitochondrial function after exposure to AraC.

To better understand why the response to AraC differed in drug-sensitive cells, we asked how TRMT5 depletion affected nascent protein synthesis in OCI-AML2 and MOLM13 cells (Figure 3L). Loss of TRMT5 caused similar changes in proteins involved in energy metabolism and the unfolded protein response (Figure 3L-N, blue circles), but the cellular response to AraC differed dramatically between the 2 KO lines (Figure 3L-N, red circles). Thus, only the mitochondria in drug-tolerant OCI-AML2 cells were capable of meeting the energy demands necessary for survival in response to AraC, but KO of TRMT5 reduced mitochondrial activity in all cells. Mitochondrial metabolism was not universally required for drug responses (supplemental Figure 3J-K; supplemental Table 10A-E). Among daunorubicin, Ven, and azacitidine (Aza), only the combination of Ven-Aza enhanced nascent mt-mRNA translation similar to AraC (supplemental Figure 3K-N; supplemental Table 11A-E).

Drug-tolerant cells withstand mitochondria inhibition only in the absence of AraC

To directly test how deletion of TRMT5 affected cell proliferation, we performed growth competition assays (Figure 4A). Although depletion of TRMT5 led to a growth disadvantage in all tested cell lines (Figure 4B-C; supplemental Figure 4A-B), the apoptosis rate was approximately fourfold higher in drug-sensitive MOLM13 cells (Figure 4D; supplemental Figure 4B). In comparison, healthy primary $CD34^+$ blood cells exhibited a twofold increase in apoptosis after TRMT5 deletion (supplemental Figure 4C-D). To track the fate of TRMT5-KO cells over time, we quantified the number of cells containing the CRISPR-induced mutations over a period of 20 days (Figure 4E-F). OCI-AML2 tolerated TRMT5 mutations for up to 17 days, but MOLM13-KO cells were eliminated after just an 8-day culture period (Figure 4E-F). Healthy $CD34^+$ progenitors demonstrated intermediate sensitivity to TRMT5 depletion between MOLM13 and OCI-AML2 cells (supplemental Figure 4E).

To test for single-cell viability, we performed colony-forming unit assays. Only drug-tolerant cells (OCI-AML2, OCI-AML3) formed colonies in the absence of TRMT5, yet their size and number were significantly reduced (Figure 4G-H; supplemental Figure 4F-K). Exposing drug-tolerant TRMT5 KO cells to AraC further decreased their survival (Figure 4I-K; supplemental Figure 4L-N). In contrast, drug-sensitive cells had equally high levels of apoptosis, whether exposed to AraC or after TRMT5 deletion (Figure 4L; supplemental Figure 4O). Accordingly, we did not observe additional proteomic alterations in AraC-exposed MOLM13 KO cells (supplemental Figure 4P; left panel). In contrast, drug-tolerant OCI-AML2 KO cells exhibited major changes in mRNA translation in response to AraC treatment (supplemental Figure 4P; right panel). In particular, expression of proteins regulating mitochondrial import and DNA damage repair was significantly altered (supplemental Figure 4Q-R).

Finally, we revealed that TRMT5-mediated mt-tRNA methylation was required for both efficient cell growth and survival in response to AraC exposure. Drug-tolerant KO cells were rescued by reexpression of the WT, but not the (mutant, ΔMTS), TRMT5 protein (Figure 4M). Similarly, the ability to withstand exposure to AraC required the formation of m^1G37 in mt-tRNAs (Figure 4N).

Our data so far revealed that drug-tolerant cells, which depend less on mitochondria for energy production under steady-state growth conditions, were less affected by TRMT5 depletion. However, the activation of mitochondrial function, and consequently the upregulation of TRMT5-driven mt-mRNA translation, was essential for survival in the presence of AraC.

TRMT5-mediated mitochondrial functions drive leukemia progression in vivo

To validate TRMT5 as a drug target in cancer therapy, we performed xenotransplantation assays using drug-tolerant and -sensitive AML cells (Figure 5A; supplemental Figure 5A-B).

Downloaded from http://ashpublications.org/blood/article-pdf/146/20/2443/2420053/blood_bld-2024-027822-main.pdf by guest on 20 March 2026

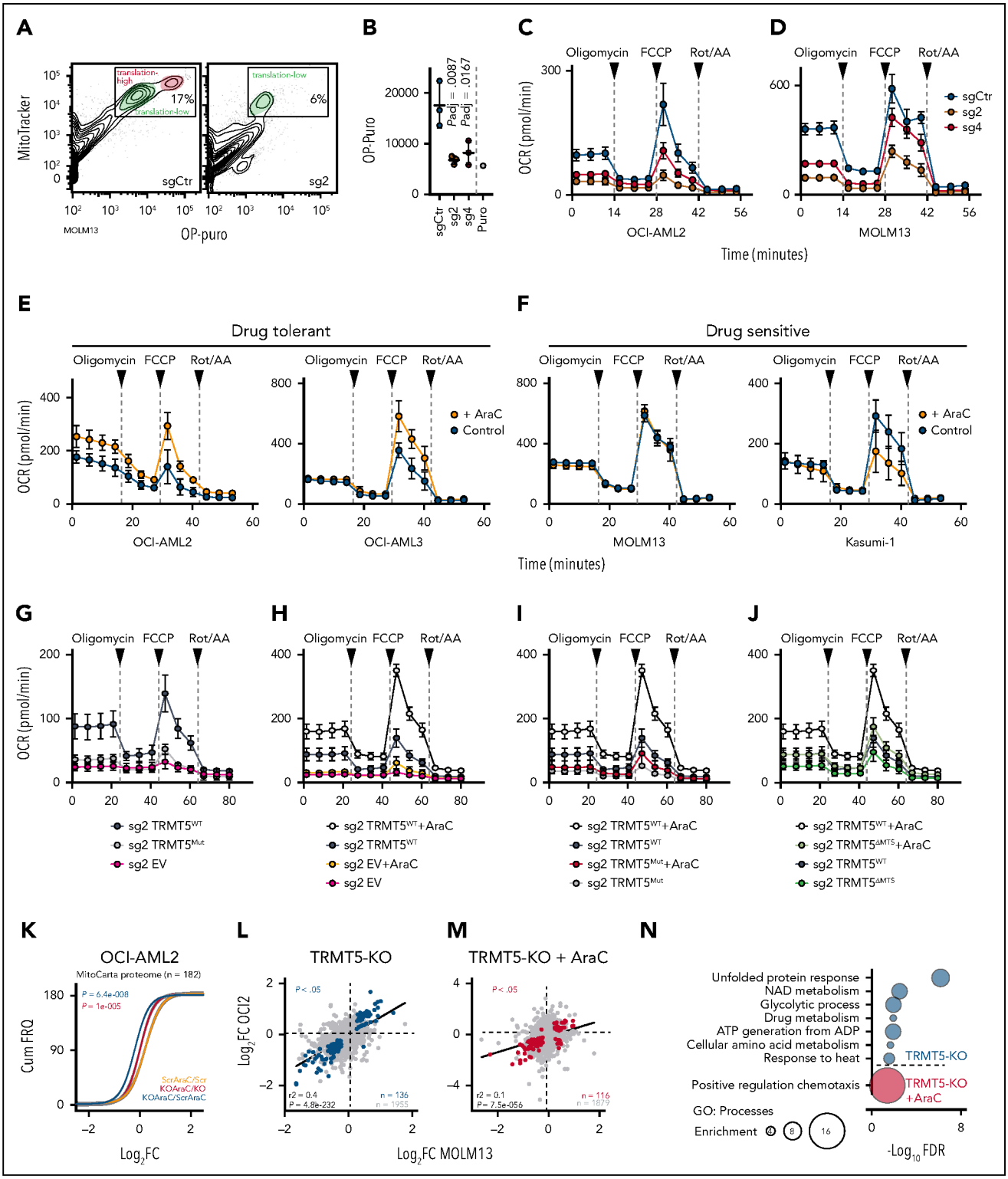

Figure 3. Drug tolerance requires switching from low to high OXPHOS in AML cells. (A-B) Flow cytometry (A) and quantification (B) of OP-puro incorporation into nascent polypeptides in mitochondria of TRMT5-depleted (sg2, sg4) and control (sgCtr) MOLM13 cells. Puromycin-treated cells served as a control. (C-D) OCR in OCI-AML2 (C) and MOLM13 (D) TRMT5 KO (sg2, sg4) and sgCtr cells. (E-F) OCR in drug-tolerant OCI-AML2, OCI-AML3 (F) and drug-sensitive MOLM13 and Kasumi-1 (F) cells exposed to cytarabine (AraC) (orange) or untreated (control) (blue). (G-J) OCR in rescued TRMT5-KO cells (sg2) using the WT, enzymatic dead MUT, mitochondria-deficient (ΔMTS) constructs of TRMT5, or the EV as control in the presence (+AraC) or absence of cytarabine. (K) Cum FRQ of $\log_2$ FC of nascent protein abundance of mitochondrial proteins (MitoCarta3.0; n = 182) in AraC-treated control (scr) OCI-AML2 cells (yellow), AraC-treated TRMT5-KO cells (red), or AraC TRMT5-KO cells vs control (scr) cells (blue). Scr: Infection of a scramble sgRNA. (L-N) Correlation of $\log_2$ FC of nascent translation in TRMT5 OCI-AML2 (OCI2) and MOLM13-KO cells in the absence (L) or presence (M) of AraC and corresponding gene enrichment analyses (N) (GOrilla). Mean ± standard deviation (panels B-J). Dunnett multiple comparison test (panel B). Wilcoxon matched-pair signed rank test (panel K). ATP, adenosine triphosphate; ADP, adenosine 5′-diphosphate; Cum FRQ, cumulative frequency; FCCP, carbonylcyanide-p-trifluoromethoxyphenylhydrazone; FDR, false discovery rate; GO, Gene Ontology; OP-puro, O-propargyl-puromycin; Rot/AA, rotenone and antimycin A.

Downloaded from http://ashpublications.org/blood/article-pdf/146/20/2443/2420053/blood_bld-2024-027822-main.pdf by guest on 20 March 2026

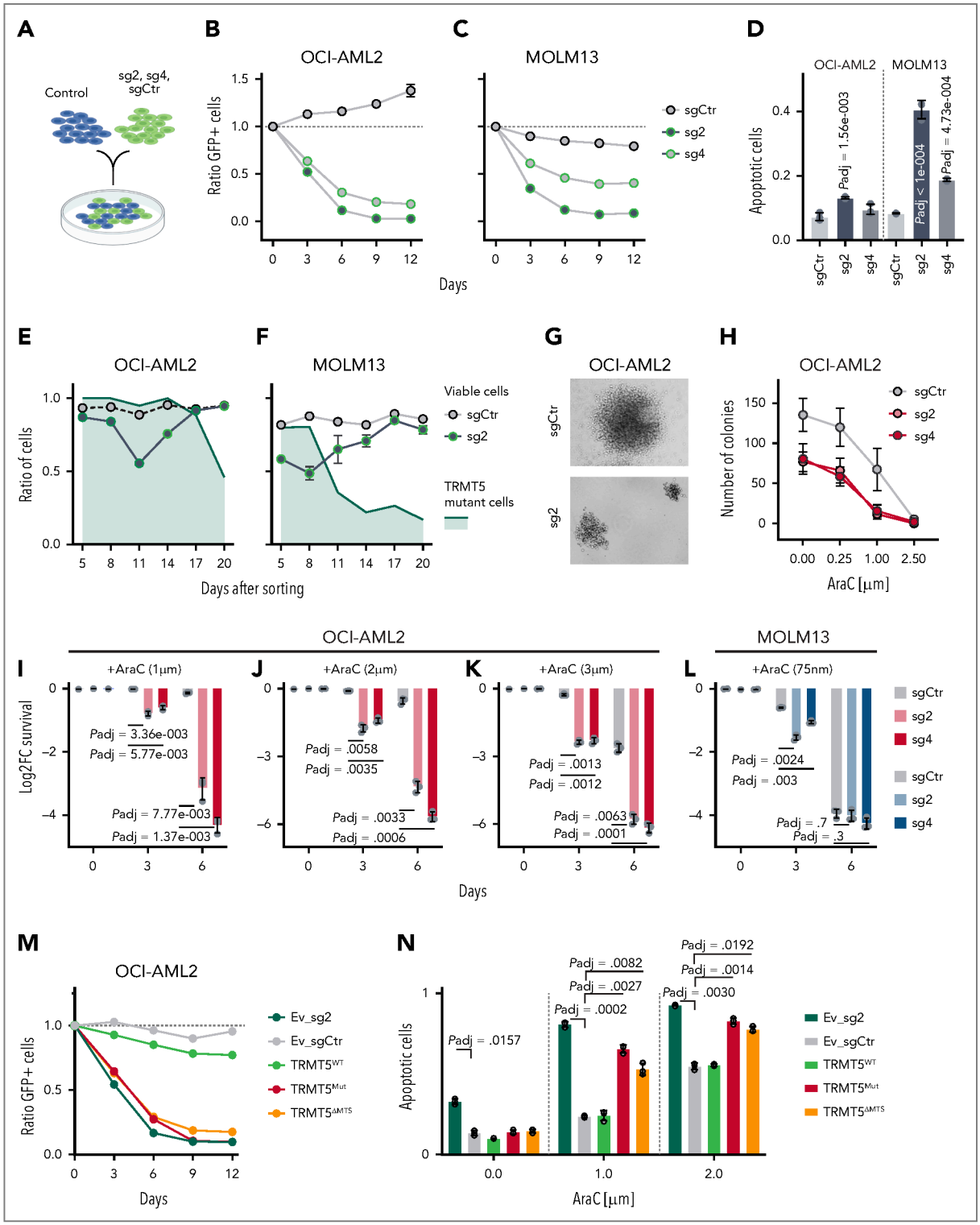

Figure 4. Drug tolerance requires m^{1}G in mt-tRNA. (A-C) Illustration (A) of growth competition assays using GFP-labelled OCI-AML2 (B) and MOLM13 (C) control (sgCtr) and KO cells (sg2, sg4). (D) Frequency of apoptotic cells in populations of OCI-AML2 and MOLM13 control (sgCtr) and KO (sg2, sg4) cells using Annexin V labelling 3 to 5 days after cell sorting. (E-F) Quantification of mutated OCI-AML2 (E) and MOLM13 (F) cells (green line) overlaid with the frequency of viable TRMT5-KO (sg2) (black dots) and control (sgCtr) (white dots) cells over time. (G-H) Representative bright field image (G) and colony-forming efficiency assays (H) of OCI-AML2 control (sgCtr) and KO (sg2, sg4) cells in the presence of increasing concentrations of AraC. (I-L) Log_2 FC of survival of drug-tolerant OCI-AML2 (I-K) and drug-sensitive MOLM13 (L) control (sgCtr) and TRMT5-KO (sg2, sg4) cells at the indicated time points. (M-N) Growth competition assay (M) and relative number of apoptotic cells after cytarabine (AraC) treatment (N) in Ctr and rescued TRMT5 KO cells. Cells were infected with a scramble (scr) or TRMT5 targeting gRNA (sg2). KO cells were rescued by reexpressing TRMT5 WT, catalytic dead (MUT) or lacking the MTS constructs. Control cells (sg2 and scr) were rescued with an EV control. Dunnett multiple comparisons test (panels D and N). Two-way analysis of variance multiple comparisons test (panels I-L).

Downloaded from http://ashpublications.org/blood/article-pdf/146/20/2443/2420053/blood_bld-2024-027822-main.pdf by guest on 20 March 2026

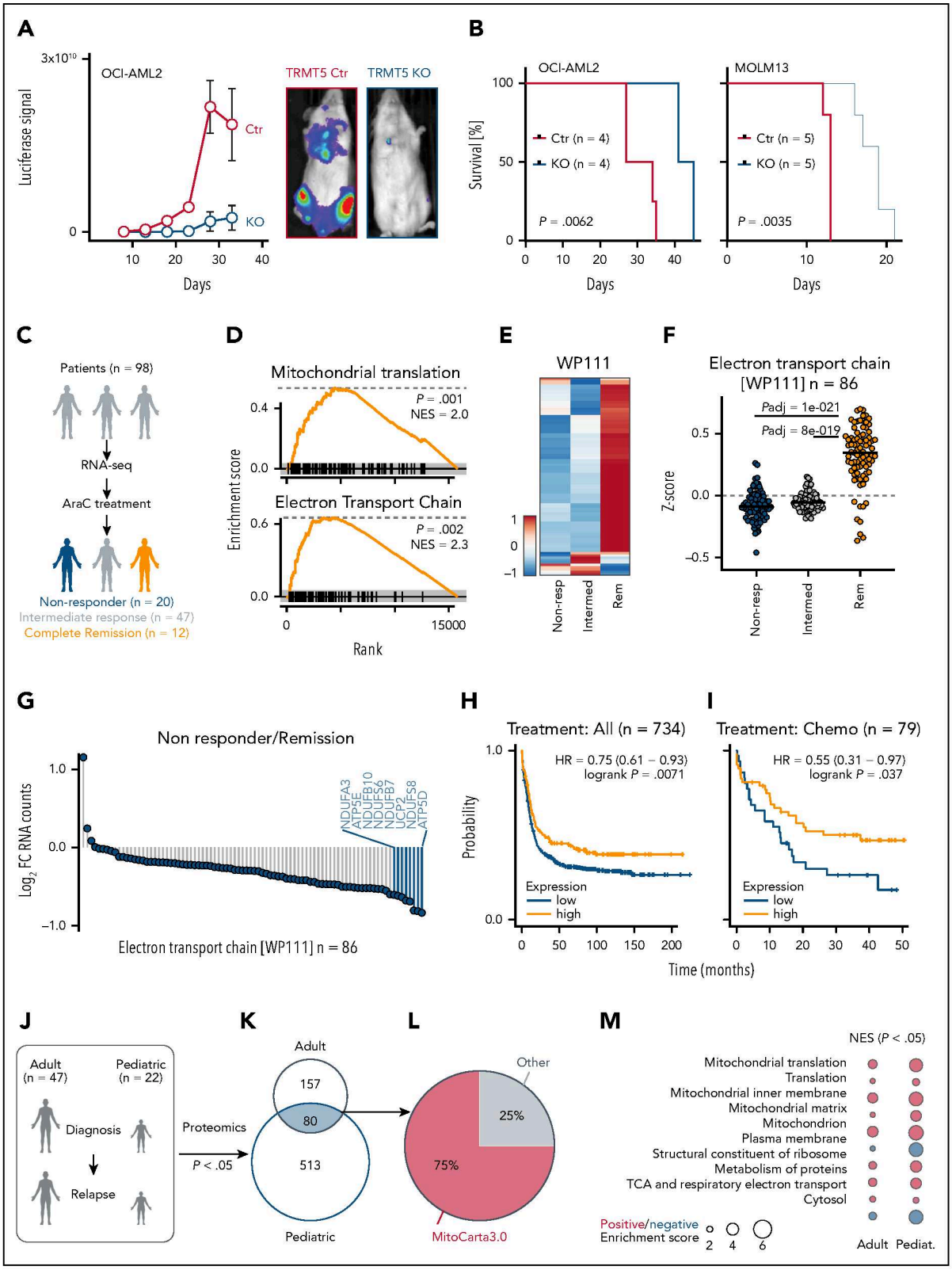

Figure 5. TRMT5 function and predictive value in leukemia. (A) Quantification (left) and representative engraftment images (right) of xenotransplanted Ctr and TRMT5-KO cells (OCI-AML2) into host mice. (B) Leukemia-free survival of mice transplanted with Ctr and KO OCI-AML2 (left) or KO MOLM13 (right) cells at the indicated time points. (C) Illustration of AML patient cohort and treatment. (D) Gene set enrichment analyses (GSEA) for genes encoding proteins regulating mitochondrial translation (top) and the ETC (bottom) using RNA expression levels of AraC treatment-responsive patients with leukemia at the time of diagnosis (n = 12) revealing complete remission (Rem) after first induction therapy. (E-F) Heat map of log_2 RNA normalized counts (ClustVis) (E) and z-score (F) of gene regulation–encoding proteins of the ETC (WP111; n = 86) in non-responders (non-resp) (n = 20), intermediate responders (n = 47), and patients having complete Rem (n = 12) at first induction therapy. (G) Average log_2 FC of normalized RNA counts of ETC genes (WP111) in patients not responding to therapy (n = 20) compared with patients having complete Rem (n = 12). (H-I) Prediction of

Downloaded from http://ashpublications.org/blood/article-pdf/146/20/2443/2420053/blood_bld-2024-027822-main.pdf by guest on 20 March 2026

The ability to initiate a leukemia was dramatically reduced in the absence of TRMT5 in both lines and enhanced survival of the mice (Figure 5B). The strict requirement of TRMT5 for successful engraftment indicated that the establishment of a leukemia requires OXPHOS for energy production[33] and is in line with elevated TRMT5 expression in human AML vs healthy tissues (supplemental Figure 5C).[34]

To test whether mitochondrial activity predicted cytarabine-based therapy outcome, we analyzed RNA sequencing data from 98 patients obtained at the time of AML diagnosis (Figure 5C).[35] After first induction therapy, we analyzed those patients who had complete remission (n = 12), no treatment response (n = 20), or an intermediate response (n = 47). RNA levels of genes encoding ETC proteins were significantly lower in patients who did not respond to therapy (Figure 5D-F; supplemental Figure 5D). To test whether low levels of OXPHOS genes were associated with poor therapy outcomes, we averaged the expression of the 7 most downregulated ETC genes (Figure 5G; blue bars). We excluded ATP5E because it lacked a JetSet probe.[36] Low average expression of the ETC genes significantly correlated with the response to induction chemotherapy (supplemental Figure 5E) but was unrelated to sex or TP53 mutation status (supplemental Figure 5F-G). The correlation between inherently low pretherapy OXPHOS levels and poorer treatment outcomes aligns with our finding that drug-resistant AML cells do not rely on OXPHOS for steady-state growth (Figure 3).

To independently validate the association between low expression of OXPHOS genes and poor therapy outcomes, we analyzed 2 additional publicly available data sets, KM-Plotter [37] and BEAT-AML.[38,39] Low average expression of the 7 ETC genes was associated with worse prognosis (Figure 5H; supplemental Figure 5H-I), and this was even more pronounced when we filtered for patients undergoing chemotherapy (Figure 5I). Multivariable analyses using clinical data from the BEAT-AML study revealed that low ETC gene expression was one of the independent variables significantly associated with shorter overall survival (supplemental Table 12). Moreover, low ETC gene expression predicted poorer outcomes specifically in patients without FLT3, IDH1, or IDH2 mutations (supplemental Figure 6A-H).

To test the role of mitochondrial function in cytarabine-treated leukemia, we analyzed proteomic data from 47 adult and 22 pediatric patients with AML at diagnosis and relapse[20] (Figure 5J). Most shared differentially expressed proteins (75%) in relapsed adult and pediatric patients localized to mitochondria (MitoCarta3.0) (Figure 5K-L) and were significantly enriched for ETC components (Figure 5M; supplemental Table 13), indicating that resistant leukemia cells underwent lasting mitochondrial metabolic reprogramming as an adaptation to therapy.

Exploiting mitochondrial vulnerabilities to enhance leukemia treatment

The active form of cytarabine, cytosine arabinoside triphosphate, is incorporated into DNA and causes DNA damage by stalling replication forks. Accordingly, we measured significant alterations in mRNA translation of genes encoding proteins involved in the DNA damage response (supplemental Figure 4R). Because mitochondria sense DNA damage signals, we asked whether their impact on cell survival during AraC treatment was indirect, via nuclear DNA damage responses.

Two lines of evidence suggested that mitochondria directly mediated cellular survival in response to chemotherapeutic drugs. First, drug-tolerant OCI-AML2 and OCI-AML3 cancer lines survived a >10-fold higher concentration of CCCP, a chemical inhibitor of oxidative phosphorylation, confirming low dependency on OXPHOS under normal growth conditions (supplemental Figure 7A). Second, cell death of TRMT5-depleted cells also increased in response to the BCL2-specific inhibitor Ven (Figure 6A-C).

BCL-2 inhibition reduces oxidative phosphorylation and selectively eradicates quiescent leukemia stem cells.[40] In addition to leukemia stem cells, we revealed that drug-tolerant AML cells require oxidative phosphorylation to survive acute stress. Therefore, we next tested whether combining Ven with TRMT5 inhibition could enhance Ven efficacy while potentially reducing toxicity. To inhibit TRMT5, we endogenously fused the *TRMT5* gene in-frame with the $FKBP12^{F36V}$ degron.[19] Treatment with dTAG-V1 reduced degron-tagged TRMT5 protein levels in a concentration-dependent manner for at least 24 hours (Figure 6D). Then, we tested how combining dTAG-V1 with Ven affected cell death and found a significant synergistic effect when the 2 drugs were used simultaneously (Figure 6E-F; supplemental Figure 7B). The synergistic effect was further enhanced when dTAG-V1 and Ven were combined with AraC in a triple-drug treatment (Figure 6G-H; supplemental Figure 7C). We observed similar synergistic effects in the OCI-AML3 drug-tolerant cell line (supplemental Figure 7D-I).

In summary, we propose that inhibition of mitochondrial functions through blocking tRNA modifications can circumvent adaptive resistance to Ven and cytarabine therapies in AML.

Discussion

Our study identifies 2 interdependent mechanisms that are essential for leukemia cells to survive cancer drug treatments. First, AML cells must contain functional mitochondria that have the capacity to upregulate metabolic pathways including OXPHOS to initiate survival. Second, this mitochondrial metabolic response requires the formation of m^1G at the tRNA anticodon loop to drive mRNA translation and boost OXPHOS.

Figure 5 (continued) survival of all patients with AML (n = 734) (H) or patients treated with chemotherapy (n = 79) (I) (kmplot.com) using the average expression of the 8 most downregulated WP111 genes in non-resp in G (blue bars): 218563_at (NDUFA3), 223112_s_at (NDUFB10), 203606_at (NDUFS6), 202839_s_at (NDUFB7), 208998_at (SLC25A8), 203190_at (NDUFS8), and 213041_s_at (ATP5D). Only JetSet probes were used. (J-K) Illustration (J) and overlap of significantly ($P < .05$) differently abundant proteins (K) of AML patient samples collected for proteomics analysis.[20] (L-M) Percentage of proteins (n = 80) in panel K localizing to mitochondria (MitoCarta3.0) (L) and GSEA analysis (https://tau.cmmt.ubc.ca/eVITTA/) revealing significantly ($P < .05$) enriched pathways in relapsed adult and pediatric (pediat.). AML samples (M). Šídák multiple comparisons test (panel F). HR, hazard ratio; NES, normalized enrichment score.

Downloaded from http://ashpublications.org/blood/article-pdf/146/20/2443/2420053/blood_bld-2024-027822-main.pdf by guest on 20 March 2026

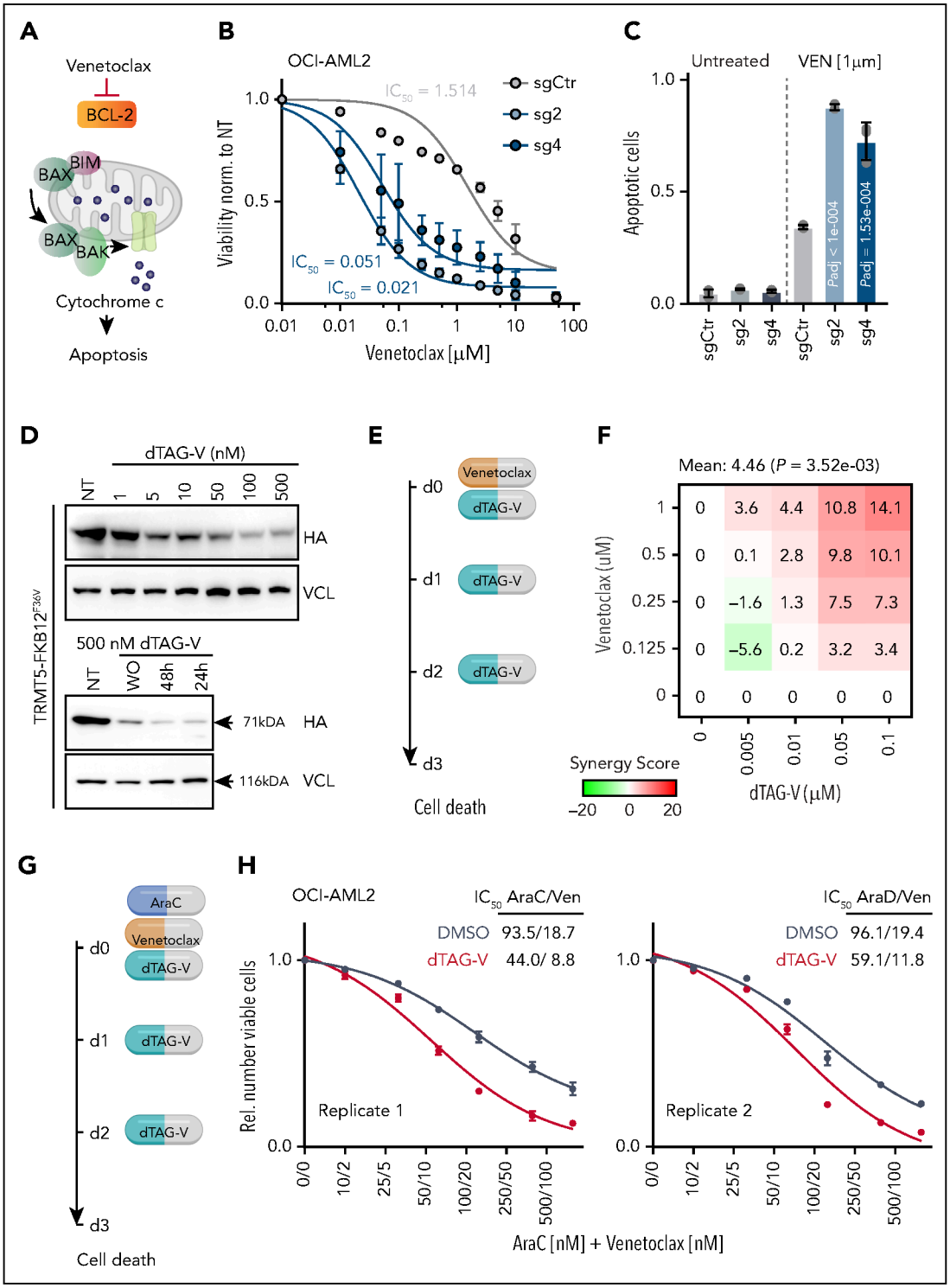

Figure 6. Exploiting mitochondrial vulnerability in therapies. (A) Illustration of Ven mechanism of action. (B-C) IC_{50} curves (B) and quantification of apoptotic cells (C) of OCI-AML2 control (sgCtr) and TRMT5 KO (sg2, sg4) cells in the presence of Ven (n = 3 biological replicates averaged over 3 technical replicates). (D) Western blot revealing protein levels of endogenously degron- and HA-tagged TRMT5 (HA) after treatment with dTAG-V1 at the indicated concentrations (top panels) or 24 and 48 hours after treatment with 500 nM dTAG-V1 (bottom panels). WO indicates washout and sample harvested after 24 hours. VCL served as loading control. (E) Illustration of combinatorial treatment of TRMT5 degron-tagged OCI-AML2 with Ven and dTAG-V1 at the indicated days (d). (F) Bliss score calculation of synergistic effect of Ven and dTAG-V1 treatment on cell death (Annexin V) at the indicated concentration. (G) Illustration of combinatorial treatment of Ven, AraC, and dTAG-V1 at the indicated days (d). (H) Synergistic effect of dTAG, Ven, and AraC on cell viability (nonlinear curve fitting). Illustrated are 2 independent OCI-AML2 tagged clones. Mean ± SD (panels B-C). Dunnett multiple comparison test (panel C). IC_{50}, 50% inhibitory concentration.

Downloaded from http://ashpublications.org/blood/article-pdf/146/20/2443/2420053/blood_bld-2024-027822-main.pdf by guest on 20 March 2026

Mitochondria are central hubs for signaling pathways that collectively help cells to recover from stress conditions.[41] They sustain energy demands by generating ATP through OXPHOS and modulate reactive oxygen species levels to prevent damage. Cancer cells rely on OXPHOS to sustain proliferative capacities, metastatic spread, resistance, and stemness. Therefore, cellular stresses that affect mitochondria need to be minimized in cancer cells to avoid activation of mitochondria-associated programmed cell death.[42] When anticancer agents target OXPHOS to induce apoptosis,[43] high OXPHOS levels at diagnosis are associated with better immediate therapy outcome in patients.

In contrast, low OXPHOS levels correlated with worse therapy outcome and enhanced drug resistance. Our data align with studies revealing that metabolic reprogramming events, which reduce mitochondrial oxidation and increase glucose, lipid, and amino acid metabolism contribute to treatment resistance.[44,45] Unlike these studies, we propose that cancer cells require metabolic flexibility to survive drug treatments and must be capable of upregulating mitochondrial functions because (1) exposure to cytarabine upregulated OXPHOS only in drug-tolerant cells and (2) inhibiting mt-mRNA translation by removing the m^1G tRNA modification resensitized drug-tolerant cells to cytarabine and Ven.

We propose that combining cytarabine, Ven, and a TRMT5 inhibitor is a promising strategy, potentially benefiting older or unfit patients with AML on Ven with low-dose cytarabine,[46] drug-resistant patients, or those experiencing severe therapy-related side effects. We also found that exposing drug-tolerant cells to Ven and Aza induces proteomic changes similar to those of cytarabine treatment, including upregulation of mitochondrial protein mRNA translation. Ven and Aza is frequently used in treatment-naive patients ineligible for intensive chemotherapy,[47] and TRMT5 inhibition may further enhance its therapeutic efficacy.

Patients with leukemia with low expression of candidate ETC genes may be ideal for stratification into combinatorial treatments, as low ETC expression was associated with worse outcomes in those with intermediate-risk karyotype and minimally differentiated AML. Our finding that low ETC gene expression correlates with worse outcomes in patients with AML without common FLT3, IDH1, or IDH2 mutations supports the hypothesis that metabolic plasticity contributes to chemotherapy resistance in tumor-persistent cells.[48] Mutations in IDH1, IDH2, and FLT3 alter metabolic profiles and potentially reduce metabolic flexibility. For example, $FLT3^{ITD}$ AML cells metabolically depend on glutaminolysis,[49] and AML cells with IDH mutations rely on enhanced mitochondrial oxidative metabolism.[50,51]

In summary, single-tRNA modifications represent promising targets for novel therapies in chemotherapy-resistant AML.

Acknowledgments

The authors thank all German Cancer Research Center (DKFZ) core facilities for their support, in particular the flow cytometry and the genomics and proteomics facilities. They extend special thanks to the Omics IT and data management core facility, the European Molecular Biology Laboratory genomics core facility, and all members of staff of the DKFZ Central Animal Laboratory.

This work was funded by the Helmholtz Association (W2/W3-106) and a Merck competitive research Drug Discovery Grant. The authors gratefully acknowledge the data storage service SDS@hd supported by the Ministry of Science, Research and the Arts Baden-Württemberg and the German Research Foundation through grant INST 35/1503-1 FUGG, and support from the German Research Foundation project numbers 439669440 TRR319 RMaP and 533056198 SFB 1709.

Some figure panels were created with BioRender.com. Frye M. (2025) https://BioRender.com/wsz4xtv.

Authorship

Contribution: C.P. and M.K. designed and performed the research, analyzed and interpreted the data, and wrote the manuscript; M.F.B., O.B., S.M.N.Z., L.W., and D.H. performed the research; C.R. and A.H.-M. analyzed and interpreted the data; F.X., K.W., S.D., N.K., K.T., D.Z., F.Z., L.L., A.O., U.P., C.B., H.S., M.B., and C.B.V. collected the data; S.A.B. contributed vital new reagents or analytical tools; J.K. and E.M.N. designed the research; C.M.-T. supervised and designed the research, interpreted the data, and contributed vital new reagents or analytical tools; and M.F. supervised and designed the research, analyzed and interpreted the data, and wrote the manuscript.

Conflict-of-interest disclosure: E.M.N. holds a patent on the nano-transfer RNAseq method (WO2024/069464A1); and is a scientific advisory board member of Immagina Biotech. The remaining authors declare no competing financial interests.

ORCID profiles: C.P., 0000-0001-8506-1571; M.K., 0009-0003-4895-9069; C.R., 0000-0001-6778-5971; D.H., 0000-0002-5047-877X; F.X., 0000-0003-3299-6415; S.D., 0000-0003-1077-829X; D.Z., 0000-0002-7602-3597; A.O., 0000-0002-2778-017X; U.P., 0000-0003-1863-3239; H.S., 0000-0001-8472-5516; M.B., 0000-0002-5916-3029; J.K., 0000-0001-7549-9326; C.M.-T., 0000-0002-7166-5232; M.F., 0000-0002-5636-6840.

Correspondence: Michaela Frye, Mechanisms Regulation Gene Expression, German Cancer Research Center, Im Neuenheimer Feld 280, 69120 Heidelberg, Germany; email: m.frye@dkfz.de; and Carsten Müller-Tidow, Department of Internal Medicine V, Heidelberg University Hospital, Im Neuenheimer Feld 410, 69120 Heidelberg, Germany; email: carsten.mueller-tidow@med.uni-heidelberg.de.

Footnotes

Submitted 8 December 2024; accepted 5 June 2025; prepublished online on *Blood* First Edition 1 August 2025. https://doi.org/10.1182/blood.2024027822.

*C.P. and M.K. contributed equally to this study.

RNA sequencing data using VDH15 cells have been deposited in the European Genome-phenome Archive (EGA) (accession number EGAS00001004765, including the attached study EGAD00001010172).

All other sequencing data have been deposited in the Gene Expression Omnibus (GEO) database (accession number GSE228208).

Nanopore transfer RNA sequencing data (base-called FASTQ and counts) have been deposited in the GEO database (accession number GSE227817; reviewer access token, ifcvykwmzjuzfqb).

The CRISPR/Cas9 genetic screening data are available at ShinyApp: https://shiny-portal.embl.de/shinyapps/app/15_rnamod_trmt5 (username, TRMT5; password, m1G). Quantitative proteomics raw data are available in supplemental Tables 7-10.

The online version of this article contains a data supplement.

There is a *Blood* Commentary on this article in this issue.

The publication costs of this article were defrayed in part by page charge payment. Therefore, and solely to indicate this fact, this article is hereby marked "advertisement" in accordance with 18 USC section 1734.

Downloaded from http://ashpublications.org/blood/article-pdf/146/20/2443/2420053/blood_bld-2024-027822-main.pdf by guest on 20 March 2026

REFERENCES

1. Delaunay S, Helm M, Frye M. RNA modifications in physiology and disease: towards clinical applications. *Nat Rev Genet*. 2024;25(2):104-122.
2. Wilkinson E, Cui YH, He YY. Context-dependent roles of RNA modifications in stress responses and diseases. *Int J Mol Sci*. 2021;22(4):1949.
3. Delaunay S, Frye M. RNA modifications regulating cell fate in cancer. *Nat Cell Biol*. 2019;21(5):552-559.
4. Frye M, Harada BT, Behm M, He C. RNA modifications modulate gene expression during development. *Science*. 2018;361 (6409):1346-1349.
5. Blanco S, Dietmann S, Flores JV, et al. Aberrant methylation of tRNAs links cellular stress to neuro-developmental disorders. *EMBO J*. 2014;33(18):2020-2039.
6. Blanco S, Bandiera R, Popis M, et al. Stem cell function and stress response are controlled by protein synthesis. *Nature*. 2016;534(7607):335-340.
7. Badjatia N, Rossi MJ, Bataille AR, Mittal C, Lai WKM, Pugh BF. Acute stress drives global repression through two independent RNA polymerase II stalling events in Saccharomyces. *Cell Rep*. 2021;34(3): 108640.
8. Wu P, Gao W, Su M, et al. Adaptive mechanisms of tumor therapy resistance driven by tumor microenvironment. *Front Cell Dev Biol*. 2021;9:641469.
9. Orsolic I, Carrier A, Esteller M. Genetic and epigenetic defects of the RNA modification machinery in cancer. *Trends Genet*. 2023; 39(1):74-88.
10. Begik O, Lucas MC, Liu H, Ramirez JM, Mattick JS, Novoa EM. Integrative analyses of the RNA modification machinery reveal tissue- and cancer-specific signatures. *Genome Biol*. 2020;21(1):97.
11. Shalem O, Sanjana NE, Hartenian E, et al. Genome-scale CRISPR-Cas9 knockout screening in human cells. *Science*. 2014; 343(6166):84-87.
12. Pauli C, Liu Y, Rohde C, et al. Site-specific methylation of 18S ribosomal RNA by SNORD42A is required for acute myeloid leukemia cell proliferation. *Blood*. 2020; 135(23):2059-2070.
13. Powell CA, Kopajtich R, D'Souza AR, et al. TRMT5 mutations cause a defect in post-transcriptional modification of mitochondrial tRNA associated with multiple respiratory-chain deficiencies. *Am J Hum Genet*. 2015; 97(2):319-328.
14. Bayne AN, Dong J, Amiri S, Farhan SMK, Trempe JF. MTSviewer: a database to visualize mitochondrial targeting sequences, cleavage sites, and mutations on protein structures. *PLoS One*. 2023;18(4):e0284541.
15. Lucas MC, Pryszcz LP, Medina R, et al. Quantitative analysis of tRNA abundance and modifications by nanopore RNA sequencing. *Nat Biotechnol*. 2024;42(1):72-86.
16. Chan PP, Lowe TM. GtRNAdb 2.0: an expanded database of transfer RNA genes identified in complete and draft genomes. *Nucleic Acids Res*. 2016;44(D1):D184-D189.
17. Cox J, Mann M. MaxQuant enables high peptide identification rates, individualized p. p.b.-range mass accuracies and proteome-wide protein quantification. *Nat Biotechnol*. 2008;26(12):1367-1372.
18. Eichelbaum K, Winter M, Berriel Diaz M, Herzig S, Krijgsveld J. Selective enrichment of newly synthesized proteins for quantitative secretome analysis. *Nat Biotechnol*. 2012; 30(10):984-990.
19. Nabet B, Roberts JM, Buckley DL, et al. The dTAG system for immediate and target-specific protein degradation. *Nat Chem Biol*. 2018;14(5):431-441.
20. Stratmann S, Vesterlund M, Umer HM, et al. Proteogenomic analysis of acute myeloid leukemia associates relapsed disease with reprogrammed energy metabolism both in adults and children. *Leukemia*. 2023;37(3): 550-559.
21. Tsherniak A, Vazquez F, Montgomery PG, et al. Defining a cancer dependency map. *Cell*. 2017;170(3):564-576.e16.
22. Ghandi M, Huang FW, Jané-Valbuena J, et al. Next-generation characterization of the cancer cell line Encyclopedia. *Nature*. 2019; 569(7757):503-508.
23. Yang WQ, Xiong QP, Ge JY, et al. THUMPD3-TRMT112 is a m(2)G methyltransferase working on a broad range of tRNA substrates. *Nucleic Acids Res*. 2021; 49(20):11900-11919.
24. Sepich-Poore C, Zheng Z, Schmitt E, et al. The $METTL_5$-$TRMT_{112}$ N^6-methyladenosine methyltransferase complex regulates mRNA translation via 18S rRNA methylation. *J Biol Chem*. 2022;298(3):101590.
25. Behan FM, Iorio F, Picco G, et al. Prioritization of cancer therapeutic targets using CRISPR-Cas9 screens. *Nature*. 2019; 568(7753):511-516.
26. Dewez M, Bauer F, Dieu M, Raes M, Vandenhaute J, Hermand D. The conserved Wobble uridine tRNA thiolase Ctu1-Ctu2 is required to maintain genome integrity. *Proc Natl Acad Sci U S A*. 2008;105(14): 5459-5464.
27. Brulé H, Elliott M, Redlak M, Zehner ZE, Holmes WM. Isolation and characterization of the human tRNA-(N1G37) methyltransferase (TRM5) and comparison to the Escherichia coli TrmD protein. *Biochemistry*. 2004;43(28):9243-9255.
28. Garnett MJ, Edelman EJ, Heidorn SJ, et al. Systematic identification of genomic markers of drug sensitivity in cancer cells. *Nature*. 2012;483(7391):570-575.
29. Vilardo E, Amman F, Toth U, Kotter A, Helm M, Rossmanith W. Functional characterization of the human tRNA methyltransferases TRMT10A and TRMT10B. *Nucleic Acids Res*. 2020;48(11):6157-6169.
30. Farge T, Saland E, de Toni F, et al. Chemotherapy-resistant human acute myeloid leukemia cells are not enriched for leukemic stem cells but require oxidative Metabolism. *Cancer Discov*. 2017;7(7): 716-735.
31. Hou YM, Masuda I, Gamper H. Codon-specific translation by m^1G37 methylation of tRNA. *Front Genet*. 2018;9:713.
32. Björk GR, Wikström PM, Byström AS. Prevention of translational frameshifting by the modified nucleoside 1-methylguanosine. *Science*. 1989;244(4907):986-989.
33. Peng M, Huang Y, Zhang L, Zhao X, Hou Y. Targeting mitochondrial oxidative phosphorylation eradicates acute myeloid leukemic stem cells. *Front Oncol*. 2022;12: 899502.
34. Bartha Á, Győrffy B. TNMplot.com: a web tool for the comparison of gene expression in normal, tumor and metastatic tissues. *Int J Mol Sci*. 2021;22(5):2622.
35. Zhou F, Aroua N, Liu Y, et al. A dynamic rRNA ribomethylome drives stemness in acute myeloid leukemia. *Cancer Discov*. 2023;13(2):332-347.
36. Li Q, Birkbak NJ, Gyorffy B, Szallasi Z, Eklund AC. Jetset: selecting the optimal microarray probe set to represent a gene. *BMC Bioinformatics*. 2011;12:474.
37. Győrffy B. Discovery and ranking of the most robust prognostic biomarkers in serous ovarian cancer. *Geroscience*. 2023;45(3): 1889-1898.
38. Tyner JW, Tognon CE, Bottomly D, et al. Functional genomic landscape of acute myeloid leukaemia. *Nature*. 2018;562(7728): 526-531.
39. Bottomly D, Long N, Schultz AR, et al. Integrative analysis of drug response and clinical outcome in acute myeloid leukemia. *Cancer Cell*. 2022;40(8):850-864.e9.
40. Lagadinou ED, Sach A, Callahan K, et al. BCL-2 inhibition targets oxidative phosphorylation and selectively eradicates quiescent human leukemia stem cells. *Cell Stem Cell*. 2013;12(3):329-341.
41. O'Malley J, Kumar R, Inigo J, Yadava N, Chandra D. Mitochondrial Stress Response and Cancer. *Trends Cancer*. 2020;6(8): 688-701.
42. Nguyen TT, Wei S, Nguyen TH, et al. Mitochondria-associated programmed cell death as a therapeutic target for age-related disease. *Exp Mol Med*. 2023;55(8): 1595-1619.
43. Yadav N, Kumar S, Marlowe T, et al. Oxidative phosphorylation-dependent regulation of cancer cell apoptosis in response to anticancer agents. *Cell Death Dis*. 2015;6(11):e1969.
44. Liu S, Zhang X, Wang W, et al. Metabolic reprogramming and therapeutic resistance in

Downloaded from http://ashpublications.org/blood/article-pdf/146/20/2443/2420053/blood_bld-2024-027822-main.pdf by guest on 20 March 2026

primary and metastatic breast cancer. *Mol Cancer*. 2024;23(1):261.

45. Qiu J, Feng M, Yang G, et al. mTOR inhibitor, gemcitabine and PD-L1 antibody blockade combination therapy suppresses pancreatic cancer progression via metabolic reprogramming and immune microenvironment remodeling in Trp53$^{flox/+}$LSL-Kras$^{G12D/+}$Pdx-1-Cre murine models. *Cancer Lett*. 2023;554:216020.

46. Wei AH, Strickland SA, Hou JZ, et al. Venetoclax combined with low-dose cytarabine for previously untreated patients with acute myeloid leukemia: results from a phase Ib/II study. *J Clin Oncol*. 2019;37(15):1277-1284.

47. DiNardo CD, Jonas BA, Pullarkat V, et al. Azacitidine and venetoclax in previously untreated acute myeloid leukemia. *N Engl J Med*. 2020;383(7):617-629.

48. Fendt SM, Frezza C, Erez A. Targeting metabolic plasticity and flexibility dynamics for cancer therapy. *Cancer Discov*. 2020;10(12):1797-1807.

49. Gallipoli P, Giotopoulos G, Tzelepis K, et al. Glutaminolysis is a metabolic dependency in FLT3^{ITD} acute myeloid leukemia unmasked by FLT3 tyrosine kinase inhibition. *Blood*. 2018;131(15):1639-1653.

50. Stuani L, Sabatier M, Saland E, et al. Mitochondrial metabolism supports resistance to IDH mutant inhibitors in acute myeloid leukemia. *J Exp Med*. 2021;218(5):e20200924.

51. Bassal MA, Samaraweera SE, Lim K, et al. Germline mutations in mitochondrial complex I reveal genetic and targetable vulnerability in IDH1-mutant acute myeloid leukaemia. *Nat Commun*. 2022;13(1):2614.

© 2025 American Society of Hematology. Published by Elsevier Inc. Licensed under Creative Commons Attribution-NonCommercial-NoDerivatives 4.0 International (CC BY-NC-ND 4.0), permitting only noncommercial, nonderivative use with attribution. All other rights reserved.

Downloaded from http://ashpublications.org/blood/article-pdf/146/20/2443/2420053/blood_bld-2024-027822-main.pdf by guest on 20 March 2026